Molecular Microbiology (2011) 80(4), 981–994 ■
doi:10.1111/j.1365-2958.2011.07624.x
First published online 4 April 2011

The *Aspergillus nidulans* CENP-E kinesin motor KipA interacts with the fungal homologue of the centromere-associated protein CENP-H at the kinetochore

Saturnino Herrero, Norio Takeshita and Reinhard Fischer*
Karlsruhe Institute of Technology (KIT) – South Campus, Institute for Applied Biosciences, Department of Microbiology, Hertzstrasse 16, D-76187 Karlsruhe, Germany.

Summary

Chromosome segregation is an essential process for nuclear and cell division. The microtubule cytoskeleton, molecular motors and protein complexes at the microtubule plus ends and at kinetochores play crucial roles in the segregation process. Here we identified KatA (KipA target protein, homologue of CENP-H) as a kinesin-7 (KipA, homologue of human CENP-E) interacting protein in *Aspergillus nidulans*. KatA located at the kinetochore during the whole cell cycle and colocalized with KipA and partially with the putative microtubule polymerase AlpA (XMAP215) during mitosis. Deletion of *katA* was lethal at 37°C and caused severe growth and morphology defects at room temperature. KipA was shown before to play an important role in growth directionality determination and our new results suggest a second function of KipA in the interaction between the microtubule plus ends and the kinetochores during mitosis.

Introduction

Molecular motors are fascinating mechanochemical enzymes, which convert chemical energy into force. They generate the movement of a wide variety of materials in eukaryotic cells and thus are involved in many different cellular and developmental functions such as organelle movement, localization of polarity marker proteins, mitosis or meiosis (Schliwa and Woehlke, 2003). The transport machinery consists of polar cytoskeletal tracks, motors as engines, ATP as fuel, accessory factors as regulators and specific cargoes. Molecular motors are classified into microtubule-dependent kinesins and dynein and actin-dependent myosins. All eukaryotes contain motors of all three classes, although the number of motors of each class varies in different organisms. In the case of kinesin, *Saccharomyces cerevisiae* harbours only six, the filamentous fungus *Aspergillus nidulans* contains 11 and mammalian genomes encode about 50 putative kinesins. Kinesins are classified into 17 different families, which used to be named after, e.g. the founding members. However, a novel nomenclature has been introduced recently and the families were distinguished by numbers. The family of conventional kinesin is therefore now called kinesin-1 family, and the Kip2 family was re-named to kinesin-7 (Wickstead and Gull, 2006).

In *S. cerevisiae* kinesin-7 (Kip2) is required for microtubule plus-end accumulation of Bik1 (CLIP-170 homologue) (Carvalho *et al.*, 2004; Wu *et al.*, 2006). In *S. pombe* kinesin-7 (Tea2) performs the same function as Kip2 in *S. cerevisiae*, the transport of a CLIP-170 homologue, Tip1, to the microtubule plus end (Browning *et al.*, 2003; Busch *et al.*, 2004). The system could even be reconstituted *in vitro,* clearly showing that no other components such as membranous vesicles are required for the transportation (Bieling *et al.*, 2007). In addition, Tea2 transports the cell end marker protein Tea1 (Browning *et al.*, 2003). Tea1 is anchored at the membrane at the growing tip through the interaction with the membrane associated Mod5 protein and forms a larger protein complex with other proteins, which ultimately recruit formin. Formin then catalyses the formation of actin cables, which serve as tracks for myosin-dependent vesicle secretion, necessary for membrane and cell wall extension (Snaith and Sawin, 2003; Snaith *et al.*, 2005). Deletion of *tea2* caused bent instead of straight-growing cells (Browning *et al.*, 2000). This phenotype is due to the lack of transportation of the cell end marker protein. In order to further unravel the polarity determination machinery, a yeast two-hybrid screening was performed using Tea2 as bait (Busch *et al.*, 2004). The authors obtained 54 candidate genes, 12 of which encoded Tip1. The other potential cargoes have not yet been described.

In *A. nidulans* kinesin-7 (KipA) is – like in *S. pombe* – involved in polarity determination (Rischitor *et al.*, 2004; Konzack *et al.*, 2005; Fischer *et al.*, 2008). In addition to Tea2, other cell end factors from *S. pombe* are also

Accepted 3 March, 2011. *For correspondence. E-mail reinhard.fischer@KIT.edu; Tel. (+49) 721 608 44630; Fax (+49) 721 608 44509.

Table 1. KipA-interacting proteins detected in the yeast two-hybrid screening.

Identification No. at BROAD Institute	Amino acids/ size of the isolated clone	No. of clones in screening	Conserved domains	Assigned function in other organisms
AN0925	958/319	4	Sac1 domain, synaptojanin like phosphatase	Control of endocytosis, cell vesicle trafficking and secretion
AN2054	642/192	4	Alk1, haspin-like kinase	Cell-cycle regulated kinase. Histone H3 phosphorylation
AN2768	245/245	1	Spc34	Dam–DASH complex subunit, a kinetochore complex
AN2886	238/238	2	CENP-H	Centromeric protein
AN10061	881/448	1	F-box domain, CAAX motif	Cell separation and septation, localizes to septa and cell tips. Recycling pathway
AN2181	112/112	5	TF2A	Transcription initiation factor IIA gamma subunit
AN4739	301/137	2	SAICAR synthetase	Purine biosynthetic pathway
AN10182	346/346	2	eIF3C, Mov34/MPN/PAD-1 family	Translation initiation factor
AN2530	182/182	1	Hsp20	30 kDa Heat shock protein
AN4594	116/22	1	20S	40S ribosomal subunit protein
AN8866	476/476	1	ACT domain	D-3-phosphoglycerate dehydrogenase
AN8953	956/119	1	Alpha glucosidase	
AN3703	95/95	1	unknown	
AN8343	136/136	1	FKBP-type	Peptidyl-propyl *cis-trans* isomerase

conserved in this filamen tous fungus. Tea1 (*A. nidulans* TeaA), Mod5 (TeaR), Tea4 (TeaC) and For3 (SepA) have been characterized and a role in determining the zone for polarized growth has been shown (Sharpless and Harris, 2002; Takeshita *et al*., 2008; Higashitsuji *et al*., 2009). However, TeaA and TeaC are apparently transported to the cortex independent of KipA (Takeshita *et al*., 2008; Higashitsuji *et al*., 2009).

Kinesin-7 is also present in mammals and other higher eukaryotes where it is called CENP-E. It is undetectable in non-dividing tissues and before late G2 in cycling cells. CENP-E accumulates at the end of G2 and is degraded after mitosis (Brown *et al*., 1994). Depletion of this kinesin causes chromosome segregation errors due to a weaker spindle assembly checkpoint (Weaver *et al*., 2003) and an impaired interaction between the centromeres and the microtubules of the mitotic spindle (Putkey *et al*., 2002). The interaction partners of the CENP-E motor protein found to date are the kinase BubR1, the spindle microtubule-associated protein CENP-F (Chan *et al*., 1998), Nuf2, a member of the Ndc80 complex (Liu *et al*., 2007), Skp1, which is implicated in CENP-E degradation after mitosis (Liu *et al*., 2006), and Mitosin/Septin 7 (Zhu *et al*., 2008). CENP-E is responsible for the localization and the activity of BubR1 at the kinetochore. BubR1 phosphorylates the checkpoint component Mad2 resulting in an arrest of mitosis in metaphase. This mitotic delay is necessary for correct attachment of the sister kinetochores to the spindle, without CENP-E the checkpoint is inactive resulting in a mis-segregation of sister chromatids (Putkey *et al*., 2002).

In order to identify kinesin-7 interacting proteins in *A. nidulans*, we performed a yeast two-hybrid assay and isolated several putative new KipA-binding proteins, one of which was KatA, a putative homologue of CENP-H. CENP-H is a constitutive component of the inner kinetochore plate and is required for the targeting of other centromeric proteins (Okada *et al*., 2006). We propose an anchoring rather than a transportation function of KipA at the kinetochore and KatA as the centromeric-interacting partner of KipA during mitosis.

Results

Yeast two-hybrid screening

In order to identify cargos for the kinesin-7 KipA we screened a cDNA library by using the Matchmaker Library Construction and Screening Kit (Clontech). We used the C-terminal half of KipA as bait in order to avoid interactions of the motor domain with cytoskeletal elements such as tubulin. The bait spans from the beginning of the coiled-coil domain to the stop codon and it was cloned into the bait vector (pGBKT7). The screening was performed twice, and ~ 90 yeast colonies were isolated, one-third of which were able to grow again in the same medium (SD-Leu-Trp-His-Ade + 2 mM 3AT) and produced a blue colour in the X-gal assay. Plasmids from these colonies were sequenced, and 14 genes identified (Table 1) (Fig. 1A). We have chosen one candidate, KatA (KipA target), for a detailed analysis. The interaction between KatA and KipA was confirmed by co-immunoprecipitation (Fig. 1B).

In order to map the interaction site of KipA, we made some overlapping deletions in the C-terminus of the KipA bait (Fig. 1A). For comparison, four further proteins, obtained after the yeast two-hybrid screening with the

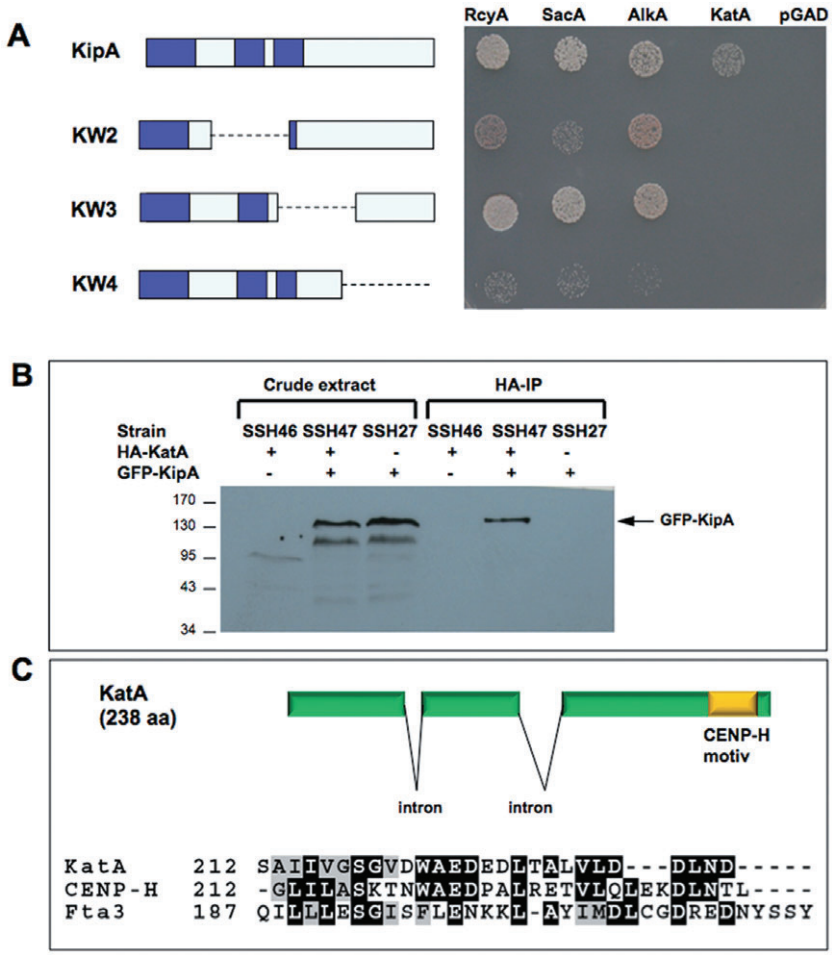

Fig. 1. Identification of KatA as interaction partner of KipA.
A. Mapping of the KipA cargo-binding domain. Yeast two-hybrid assay of KipA variants (depicted on the left) and the cargo proteins (indicated on the right). The KipA variants were cloned into the plasmid pGBKT7 (Clontech) and transformed into the *S. cerevisiae* strain AH109. Transformed yeast was crossed to the compatible strain Y187 containing the corresponding KipA-binding protein indicated above. After mating, 10 µl drops of yeast suspension with an OD_{600} of 0.1 were inoculated on a SD-Leu-Trp-His 2 mM 3AT plate and incubated at 30°C for 48 h. The blue boxes indicate the coiled-coil domains.
B. Co-immunoprecipitation of KatA and KipA. Western-blot with anti-GFP antibody of the probes indicated above the panel. Mycelium of the strains SSH27 (GFP–KipA), SSH46 (3xHA–KatA) and SSH47 (both) was cultivated at 37°C for 28 h in Thr-supplemented medium. GFP–KipA was co-precipitated with HA–KatA using the anti-HA antibody.
C. CustalW alignment of *A. nidulans* KatA, human CENP-H and *S. pombe* Fta3. Identical amino acids were shaded in black and similar amino acids are in grey. The sequence comparison is restricted to the region similar to CENP-H detected by the Pfam software (http://pfam.sanger.ac.uk/). Scheme of the exons of the *kat*A gene (green) and the position and size of the CENP-H motif (yellow).

full-length bait, were included into the study as KipA-binding partners. RcyA corresponds to AN10061, SacA to AN0925, AlkA to AN2054 and KatA to AN2886 (for more details see Table 1). The yeast two-hybrid assay between these proteins and the *kipA* deletion mutants showed that the cargo-binding domain is located at the C-terminus (Fig. 1A, KW4). Deletion of the coiled-coil domain (Fig. 1A, KW2) also affected the interaction with RcyA, SacA and AlkA, suggesting that the region is necessary to keep the conformation of the cargo-binding domain. KatA interacted only with the full-length bait. In this series of experiments KipA self-interaction was also observed (data not shown). This is consistent with the current model for kinesin motor proteins, which proposes that dimerization through coiled-coil regions is necessary for the progression along the microtubule lattice.

KatA is the fungal homologue of the centromeric protein H (CENP-H)

The *katA* cDNA was found twice in the *kipA* screening as full sequence including 5′ and 3′ UTRs. The ORF has a length of 717 bp and codes for a polypeptide of 238 amino acids. The predicted two introns of 45 and 69 bp, respectively, were confirmed by cDNA sequencing (Fig. 1C). Database searches with the KatA protein revealed that the protein is conserved in filamentous fungi, none of which has been analysed before. ClustalW analysis of KatA showed that the best-conserved region was a motif close to the C-terminus (Fig. 1C). BLAST searches at the GeneDB revealed that the most similar protein in *S. pombe* is SPAC17H9.06c (*e*-value 0.00047). This is a hypothetical protein of 601 amino acids. The second one, with an *e*-value of 0.0022, was SPBP8B7.12c, which has been characterized as Fta3/Sma3 (Liu *et al.*, 2005). Fta3 has a similar size as KatA (220 amino acids) and is associated to the Sim4 and Mal2 centromeric complex. Further analysis of KatA at the Pfam website indicated the presence of a partial CENP-H motif close to the C-terminus corresponding to the sequence 214-I**I**VGSGVD**WA**E**D**EDE**L**TALV**L**-233 (key residues in bold). This motif spans the same region that is best conserved in comparison with other filamentous fungi, and both are indicated in the alignment in Fig. 1C. In the alignment of

KatA with the human CENP-H and *S. pombe* Fta3 the key residues are better conserved in *A. nidulans* than in *S. pombe*. In a recent analysis *S. pombe* Fta3 has been assigned as CENP-H homologue whereas before Sim4 was considered as homologue of CENP-H (Pidoux *et al*., 2003; Meraldi *et al*., 2006; Przewloka and Glover, 2009). In any case Fta3 is also associated to the Sim4 complex (Liu *et al*., 2005).

CENP-H is an essential protein in human (Orthaus *et al*., 2006) and chicken cells (Fukagawa *et al*., 2001). It is a constitutive component of the inner kinetochore plate and is required for the targeting of other centromeric proteins. Although it was proposed that CENP-E, the vertebrate homologue of kinesin KipA, bridges the spindle microtubules to the kinetochore inner plate (Yao *et al*., 1997; Kim *et al*., 2008), to date it was not found which kinetochore protein is the direct partner of CENP-E at the inner plate. We propose that KatA serves this function and is the kinetochore anchor for KipA in *A. nidulans.* To proof such a function, we studied the localization of KatA.

KatA localizes in the mitotic spindle

KatA was tagged at the N-terminus with GFP, integrated at the *katA* locus and expressed from the native promoter or the *alcA* promoter with moderate induction (*Experimental procedures*). We confirmed that the localization of KatA is identical in both cases (Fig. S1). For further investigations, the transformants expressing GFP–KatA from the *alcA* promoter were analysed. The GFP–KatA fusion protein appeared as dots distributed regularly along the hyphae KatA was tagged at the N-terminus with GFP, integrated at the *katA* locus and expressed from the *alcA* promoter with moderate induction (*Experimental procedures*). In the transformed hyphae, the GFP–KatA fusion protein appeared as dots distributed regularly along the hyphae. The dots corresponded to nuclei (Fig. 2A). The GFP–KatA dots localized to the periphery of the nucleus close to the nuclear envelope, as shown in a strain with mRFP1–KatA/GFP–nup49, a marker for the nuclear pore complex (Fig. 2B) (kindly provided by S. Osmani) (Liu *et al*., 2009). The same localization pattern was observed when KatA was expressed from the natural promoter (Fig. S1).

In order to study further KatA during mitosis, we crossed strain SSH16 (mRFP1–KatA) to a strain with GFP-labelled microtubules to visualize the mitotic spindles. In *A. nidulans*, the mitotic spindle appears as compact microtubule bundle, short and thick at the beginning of mitosis and long and thin during telophase. At the beginning of mitosis (prophase-metaphase), KatA was distributed along the spindle in a dot-like pattern with the main population of the protein at the middle of the spindle (Fig. 3A, upper row). During late mitosis (anaphase-telophase), KatA disappeared completely from the equator of the spindle and

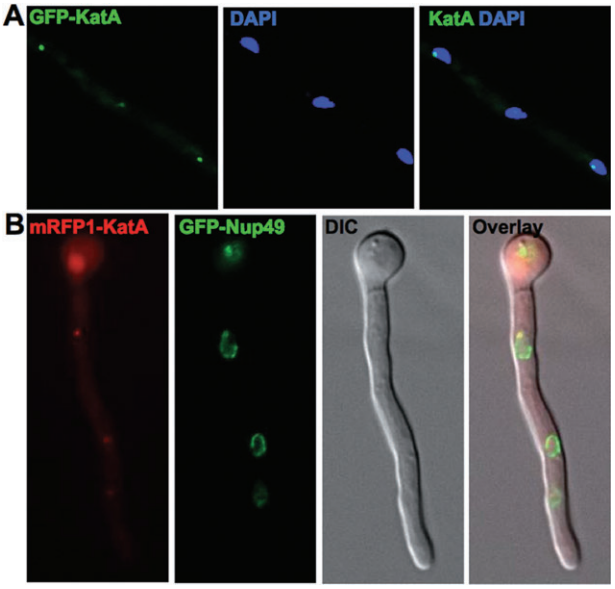

Fig. 2. Localization of KatA during interphase.
A. Strain SSH04 was grown on minimal medium with glycerol as a carbon source and stained with DAPI. KatA localized at the nucleus as shown in the DAPI stained hyphae. GFP-tagged KatA appeared associated to a single cluster in every nucleus.
B. The mRFP1-tagged KatA cluster localized at the periphery of the interphase nucleus, close to the nuclear envelope. The nuclear pore complexes are visualized with Nup49-GFP. Hyphae have a diameter of 2–3 μm.

appeared as a couple of dots segregated at the spindle poles (Fig. 3A, lower row). This dynamics is typical for centromeric DNA and kinetochore proteins (Sanchez-Perez *et al*., 2005). The same localization of KatA was found when expressed from the natural promoter (Fig. S1). Next, we have chosen AlpA as another marker for the mitotic spindle. AlpA is a microtubule-associated protein homologous to Dis1/XMAP215. It localizes at the microtubule-plus end during interphase and is probably involved in microtubule polymerization (N. Takeshita *et al*., pers. comm.) (Enke *et al*., 2007). We observed a weak AlpA signal in metaphase at the mid-zone of the spindle, exactly in the same position where the mRFP1–KatA signal was strong (Fig. 3B, metaphase). After that, AlpA appeared to dissociate from the microtubules and localized to four or five dots along the spindle (Fig. 3B, anaphase) (Enke *et al*., 2007). This pattern has previously also been described in fission yeast (Garcia *et al*., 2001). The central dots, which colocalized with KatA, correspond to the kinetochores and the distal ones are probably associated to the spindle pole bodies (SPBs). During telophase, a rest of AlpA, associated to the microtubules was again visible while the main part was concentrated at the spindle poles (Fig. 3B, telophase).

In *S. pombe* the AlpA homologue Alp14 has been described as kinetochore-associated protein (Garcia

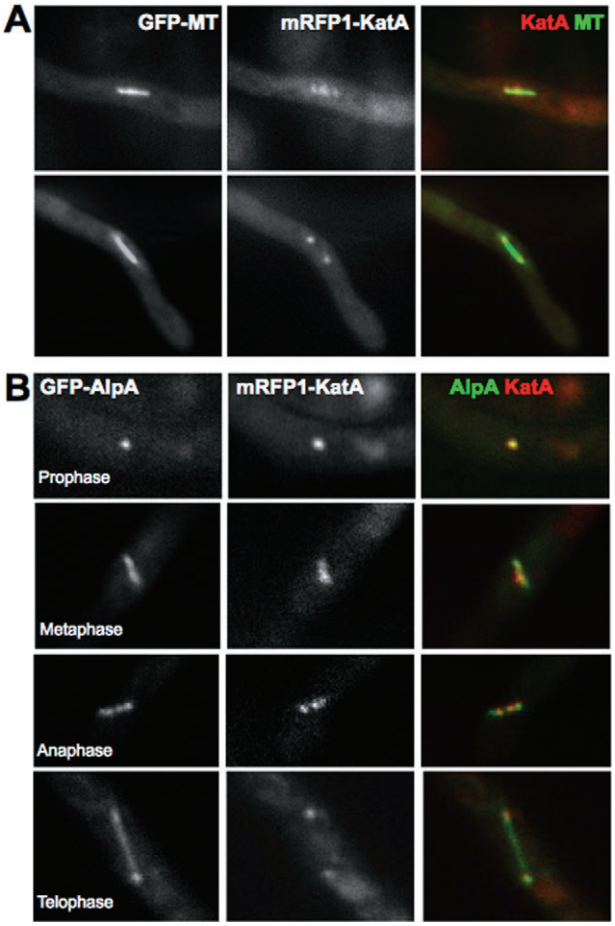

Fig. 3. Localization of KatA during mitosis.
A. Colocalization of GFP-α-tubulin-tagged microtubules and mRFP1–KatA during metaphase (upper row) and anaphase-telophase (lower row). Fluorescence images of the mitotic spindle in SSH18. Spores were incubated overnight in minimal medium with 2% glycerol.
B. Colocalization of AlpA and KatA. Fluorescence images of the mitotic spindle in SSH20 during different phases of mitosis. Spores were incubated with minimal medium with 2% glycerol in a FluoroDish tissue culture dish. Hyphae have a diameter of 2–3 μm.

et al., 2001). Therefore, we studied also the functional relation between AlpA and KatA. To test for genetic interaction of *alpA* and *katA* in *A. nidulans*, we constructed a double-mutant strain. Depletion of KatA in combination with deletion of *alpA* had an additive effect and only very small colonies were formed (data not shown).

KatA localizes at kinetochore clusters

The subcellular localization of KatA at nuclei during interphase was reminiscent of SPBs. To test this localization, we expressed mRFP1–KatA along with GFP–ApsB (Veith *et al.*, 2005) as a marker for SPBs and analysed the signals. KatA localized close to ApsB, but the signals did not overlap suggesting distinct structures (Fig. 4A). It has been described that the kinetochores of the eight chromosomes of *A. nidulans* appear as a single cluster during interphase (Yang *et al.*, 2004). This cluster is tightly associated to the SPB (De Souza *et al.*, 2009). The GFP–KatA signal thus could represent the kinetochore cluster. The localization of KatA in a cluster close to SPBs and the analysis of the protein sequence indicate that KatA is a kinetochore protein homologous to CENP-H.

In order to test whether KatA indeed is a kinetochore component in *A. nidulans,* we compared the KatA localization with the kinetochore marker SpcA. SpcA is a Spc34 homologue, which is a well-conserved kinetochore protein only found in fungi and is part of the Dam–DASH complex. This complex forms a 16-mer ring around the microtubule lattice at the kinetochore (Miranda *et al.*, 2005). Interestingly, SpcA was also isolated in our yeast two-hybrid screening as interacting protein of KipA (Table 1). Full-length SpcA was cloned as GFP-fusion protein under *alcA* promoter control and transformed in *A. nidulans*. In contrast to KatA, and according to the model of microtubule-induced self-assembly of the Dam–DASH ring complex at the kinetochore (Wang *et al.*, 2007), SpcA was not detectable in interphase. During mitosis, however, SpcA was found in the nucleus as dots like mRFP1–KatA (Fig. 4B). GFP and mRFP1 signals overlapped during metaphase-anaphase (upper row) as well as at the end of mitosis prior to disassembly or degradation of the DASH complex (lower row). At the end of mitosis only one SpcA spot was detected

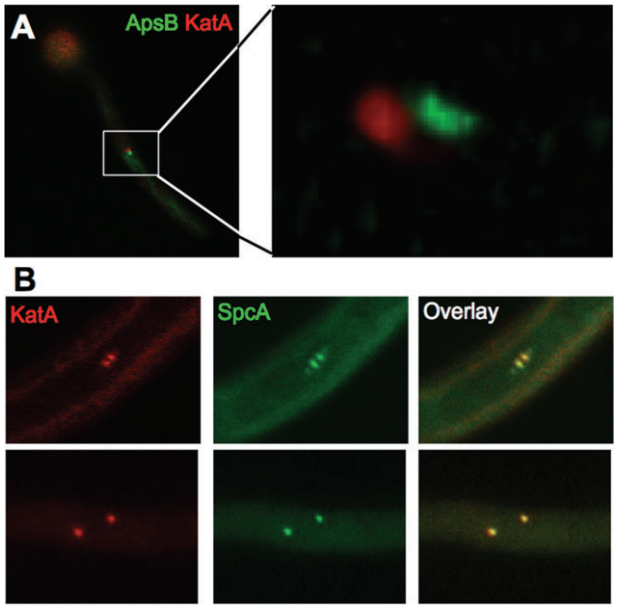

Fig. 4. KatA localizes in the vicinity of the SPB during interphase.
A. Comparison of the localization of the spindle pole body (SPB) protein ApsB (GFP) and KatA (mRFP1). The insert was enlarged to show the distinct localizations.
B. Localization of the kinetochore protein GFP–SpcA, and mRFP1–KatA (strain SSH38) during metaphase (upper row) and anaphase (lower row). Hyphae have a diameter of 2–3 μm.

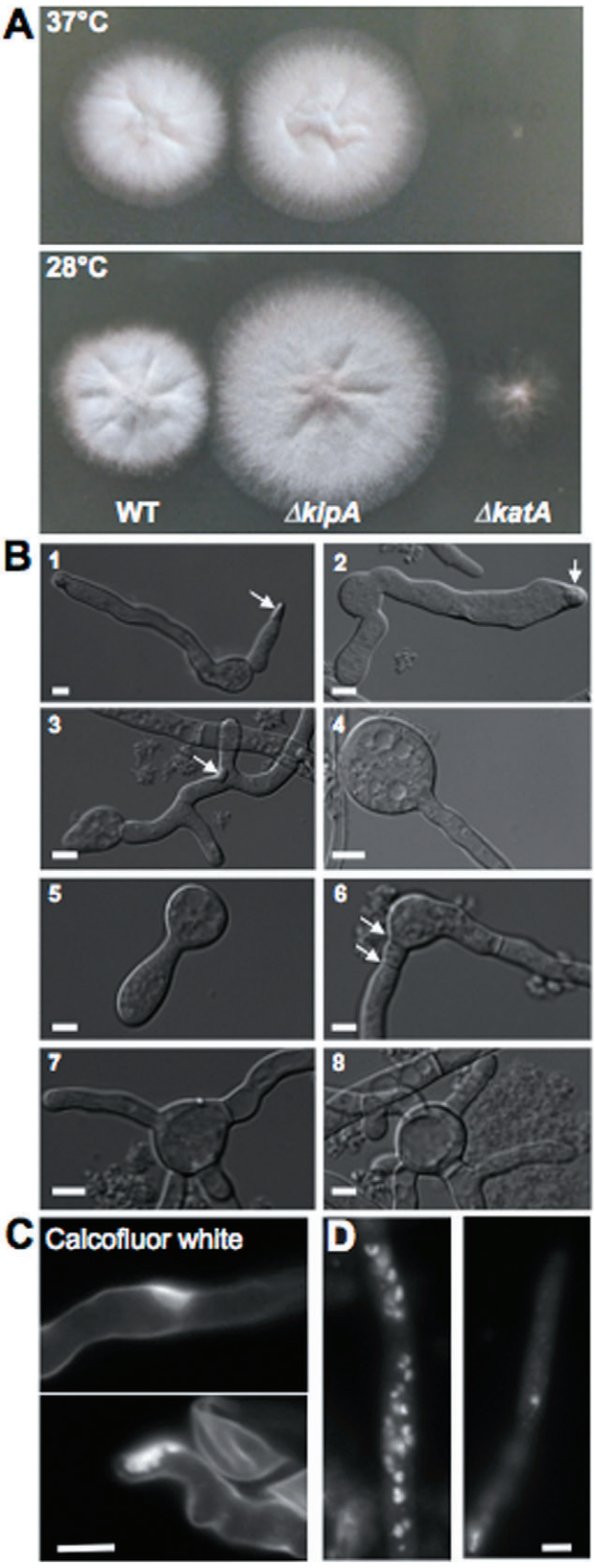

Fig. 5. Phenotype of a *kat-A* deletion strain.
A. Colony phenotype of wild-type (SO451), *ΔkipA* (SSK44) and *ΔkatA* (SSH29) strains. Complete medium agar plates were incubated for 48 h at 37°C or 72 h at 28°C.
B. DIC images of germlings of the *ΔkatA* mutant. Spores were incubated overnight at RT on coverslips with 0.5 ml of complete medium. Size bars are indicated in the figure.
C. Fluorescence images of the cell wall of SSH29 (Δ*katA*) stained with Calcofluor white. Probes were incubated for one day on complete medium. Calcofluor white was added at 2 μg ml^{-1} five minutes before the microscopy.
D. Nuclear number and distribution were highly variable in different hyphae of the *ΔkatA* mutant. Nuclei were stained with DAPI. Size bars represent 5 μm.

at each nucleus (Fig. 4B, lower panels; and Fig. S2). The fact that KatA was detectable during all cell cycle phases indicates that kinetochore association of KatA is independent of the interaction of the kinetochore with microtubules, and strengthens the idea that KatA is a homologue of CENP-H, a kinetochore protein closely associated with the centromere.

katA *is an essential gene*

In order to determine the function of *katA,* we aimed to construct a *katA* deletion strain. We were not able to obtain such a strain with our standard methods. However, we found that strains expressing KatA under *alcA*-promoter control grew more slowly under repressing conditions. Therefore, we anticipated that *katA* is an essential gene and used the heterokaryon rescue technique to obtain a knock-out strain (Osmani *et al.*, 2006a). We transformed protoplasts with the deletion cassette (Fig. S3A). Deletion of *katA* was confirmed by Southern blot (Fig. S3B). Heterokaryotic transformants grew normal but single-cell spores obtained from the heterokaryon could not grow on selective medium at 37°C (Fig. 5A) or in minimal medium at any temperature (data not shown). Conidiospores were only able to form small colonies with few conidia at low temperature in complete medium. These results suggest that deletion of *katA* is temperature-sensitive lethal at 37°C and growth is largely affected at room temperature. The residual growth at low temperature allowed us to study the cellular effects of the deletion in detail.

KatA depletion causes pleiotropic changes in hyphal morphology

Microscopic inspection of germinated spores of the *ΔkatA* mutant revealed multiple growth defects and many aberrant forms. Some of the hyphae appeared normal, others displayed an irregular width (Fig. 5B, panels 1, 2 and 5). In addition, the morphology of nuclei was altered. In many cases, nuclear distribution along the hyphae was like in wild-type. In other hyphae the number, distribution and

size of the nuclei varied largely. We observed that abnormal nuclear localization is usually accompanied by aberrant hyphae. We observed an abnormal accumulation of cell wall material at the tips and along hyphae (see arrows at panels 1, 2 and 3, Fig. 5B), which were stained with Calcofluor white (Fig. 5C). Septation was also highly abnormal with regards to the form and spacing of septa, in addition, some hyphae were without any septa (Fig. 5B, panels 2, 4 and 5). Some germinated spores were very large (Fig. 5B, panels 4 and 5), suggesting uncontrolled isotropic growth prior to or after germ tube formation. However, we observed also conidiospores with abnormal size in spore suspensions obtained from colonies on agar plates (data not shown), suggesting uncontrolled growth during spore formation. Furthermore, deletion of *katA* affected polarity initiation. In wild-type, spores form a single germ tube and a second one at the opposite site. In contrast, *ΔkatA* spores produced three, four or even five germ tubes at random positions (Fig. 5B, panels 7 and 8). Nuclear number and distribution were also highly variable in different hyphae (Fig. 5D). The role of KatA in hyphal growth was also studied in a strain where *katA* was placed under the control of the *alcA* promoter (SSH04). Conidia were germinated in glucose-containing media (repressing conditions) at 37°C and germlings observed in the microscope. As in the case of the *katA* deletion strain, misshapen germlings were observed, although the number was lower and the phenotype less severe (Fig. S4). This may be explained by residual amounts and the stability of the KatA protein in conidia. At room temperature no phenotype was visible.

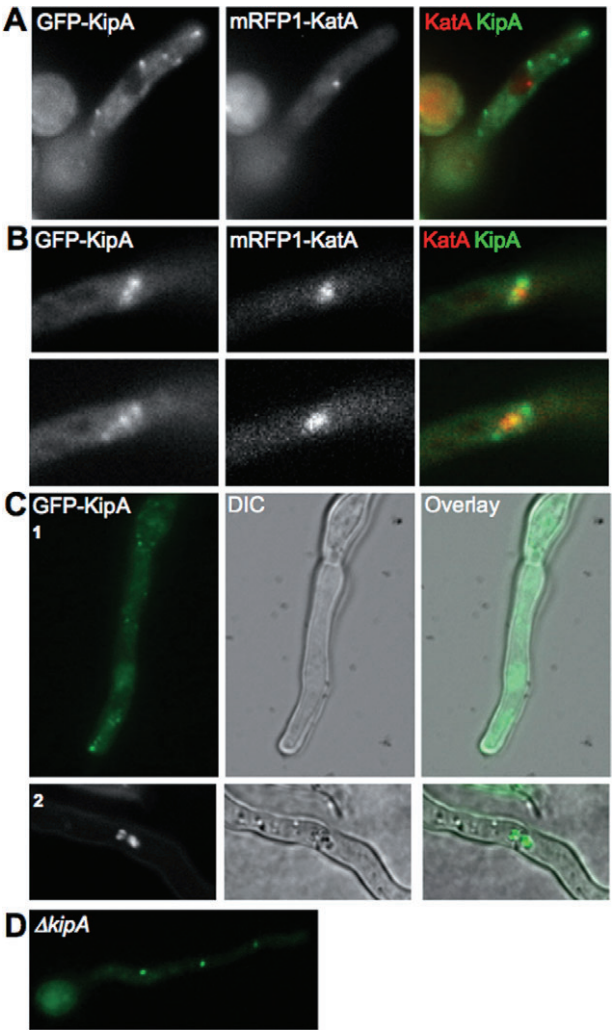

Fig. 6. Colocalization of KipA and KatA.
A. Fluorescence microscopy images of strain SSH25, which expresses GFP–KipA and mRFP1–KatA.
B. Localization of GFP–KipA and mRFP1–KatA at the mitotic spindle in strain SSH25.
C. Localization of GFP–KipA in the *ΔkatA* background. A piece of agar from the colony border of strain SSH31 was placed on a coverslip with complete medium containing 2% glycerol and incubated for one day.
D. GFP–KatA localization in strain SSH11 (*ΔkipA*).

KipA colocalizes with KatA in the spindle equator

To study the relation between KipA and KatA, we studied their localization in dependence of each other. We crossed the strains SSH16 (mRFP1–KatA) and SSK92 (GFP–KipA) and obtained strain SSH25 with both proteins tagged. In interphase, KipA localized at growing microtubule plus ends as previously described (Konzack *et al.*, 2005), and KipA was absent from the nucleus (Fig. 6A). In comparison, the location of KatA was restricted to the kinetochore with a weak signal in the entire nucleus (Fig. 6A).

At the mitotic spindle, KatA was observed at the kinetochores while GFP–KipA stained the entire spindle (Fig. 6B). However, KipA was not regularly distributed along the spindle. It was mainly located at the spindle poles and at the equator where it colocalized with KatA. The localization of KipA at the extreme of the spindle corresponded to the SPBs as shown by KipA comets, which indicate growing microtubule plus ends of astral microtubules and which originated from these points (movie 1). The localization at the middle of the spindle suggests that the interaction between KipA and KatA take place at the kinetochores during mitosis.

To study the localization of KipA in the absence of KatA, we crossed the deletion strain SSH29 with SSH27, which expresses the GFP-tagged KipA and obtained strain SSH31. The colonies with a *ΔkatA* phenotype expressing GFP–KipA were not able to form conidiospores in glucose-supplemented medium. As previously described for the *ΔkatA*-hyphal morphology, KipA localization was sometimes similar to wild-type (Fig. 6C, movie 2) or strongly altered. The KipA signal was very different in

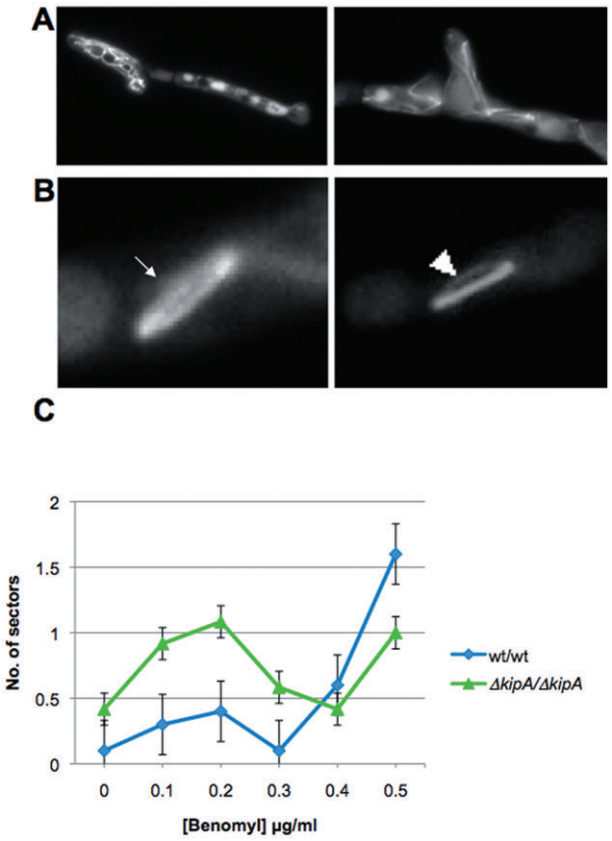

Fig. 7. Effect of *katA* deletion on the microtubule cytoskeleton and the frequency of chromosome loss.
A. Microtubule shaping in the SSH33 strain (GFP-MT, *ΔkatA*) during interphase.
B. Secondary bundles of microtubules observed in SSH33 at the mitotic spindle with free end (arrow) or bound to both poles (arrowhead).
C. Quantification of the haploidization events at increasing concentrations of benomyl indicated in the graphic. The graphic represents the number of white or yellow sectors in the colonies of diploid strains after 2 weeks at 37°C. Ten colonies of the *kipA/kipA* strain and 12 of the *ΔkipA/ΔkipA* were grown on plates with MM supplemented with the auxotrophic markers present in the parental strains.

intensity and localization in every hypha and even in different compartments of the same hypha. Because the location of KipA depends primarily on microtubules, the delocalization of the kinesin in the *katA* deletion mutant is primarily the result of changes in the cytoskeleton observed in Fig. 7A.

In contrast to the dependence of correct KipA localization on KatA, KatA localization appeared to be unaffected in the absence of KipA (Fig. 6D). As suggested previously KatA seems to be tightly associated to the centromere even in interphase when the microtubules and KipA are absent from the nucleus. The interaction between both proteins was analysed by bimolecular–fluorescence complementation (BiFC) (data not shown). The YFP signal was observed at the kinetochore clusters during interphase, although KipA alone has never been observed in the nucleus during interphase. While our data support a KatA–KipA interaction, the persistent presence of KipA in the kinetochore in interphase, and through the cell cycle, is likely an artefact due to the interaction between the two halves of YFP being irreversible.

Frequency of chromosome loss in diploid strains

To investigate an effect of *katA* deletion on nuclear division, we compared the wild-type and the *ΔkatA* mutant for the integrity of the MT cytoskeleton and chromosome loss during mitosis. In the *katA* knock-out strain the organization of the microtubule cytoskeleton was severely altered (Fig. 7A). Microtubules appeared with slightly modified lengths or distribution in some hyphal compartments. In other compartments an ordered microtubule array was completely absent and sometimes no GFP signals were observed at all. These alterations probably explain the strong effects of the *katA* deletion on hyphal morphology described in Fig. 5B. Deletion of *katA* affected also the morphology of the mitotic spindle. Instead of compact spindles, additional microtubule bundles were observed. They had a free end (Fig. 7B, left panel) or were connected to both poles giving the spindle the appearance of a security needle or a bow (Fig. 7B, right panel).

To study the effect of the *kipA* deletion on chromosome loss, we used a diploid strain. Diploid spores are formed at a low frequency and can be obtained from conidia that are generated in a heterokaryon. A diploid strain is stable when the selection pressure is maintained. In the absence of the selection pressure chromosome loss can be observed by using spore colour markers. Chromosome loss can be stimulated by the application of low concentrations of benomyl and can be visualized by the formation of sectors or colony areas with different spore colours (Rischitor *et al.*, 2004). For the present study we crossed the strains GR5 (white conidia) and RMS011 (yellow conidia) and selected a diploid with the *kipA* wild-type copy (*kipA*/*kipA*, green conidia). The *ΔkipA* strain SS44 (white conidia) was also crossed to RMS011 to obtain the heterozygous strain, *kipA/ΔkipA*. A homozygous *ΔkipA* diploid strain was generated by crossing SSK44 to GR5 and RMS011 to obtain *ΔkipA* strains with the appropriate colour and auxotrophic markers. Those strains were crossed to obtain the *ΔkipA/ΔkipA* strain. We compared the frequency of haploidization by counting the number of sectors with different colour (Fig. 7C). The number of haploidization events was very low, less than one per colony. The number of sectors increased at benomyl concentrations of 0.4 and 0.5 µg ml^{-1}. The number of sectors at low concentrations of benomyl was slightly higher in the *ΔkipA/ΔkipA* strain than in the wild-type (Fig. 7C). This suggests a role of KipA during mitosis. This finding is

further supported by the finding that in a Δ*kipA*Δ*kipB* double mutant spindles with an abnormal shape have been observed, although at low frequency (Fig. S5).

Discussion

The motor protein kinesin-7 is a component of the centromere-kinetochore interaction machinery in vertebrates and is involved in the determination of growth directionality in yeast and filamentous fungi. To date, there was no report about the function of a CENP-E-homologue in polar growth and there was no evidence for the presence of the yeast CENP-H homologue, Kip2, in the nucleus. In *A. nidulans* KipA is involved in polarity maintenance and the protein localized also in the mitotic spindle (Konzack *et al*., 2005). However, the exact function of KipA in mitosis remained elusive. In the present work, we identified KatA, a KipA-binding protein, as the CENP-H homologue in *A. nidulans*. In addition, our results suggest that mammalian CENP-E may connect mitotic microtubules to the inner plate of kinetochores through interaction with CENP-H.

The depletion of CENP-H in vertebrate cells is lethal because of aberrant chromosomes and mis-segregation of chromatids (Fukagawa *et al*., 2001; Orthaus *et al*., 2006). In *A. nidulans* deletion of *katA* caused a temperature-sensitive phenotype. Whereas at high temperature no growth was observed, small colonies were produced at lower temperatures. At permissive conditions, pleiotropic phenotypes were observed, which may be explained through the main role of KatA during mitosis. The altered morphology of the mitotic spindle (Fig. 7B) in the Δ*katA* mutant supports the idea of abnormal nuclear divisions. *A. nidulans* is a syncytial organism and the loss of one chromosome could be compensated by its presence in a neighbour nucleus. However, after a couple of nuclear divisions the gene dosage of an increasing number of genes must be altered and probably causes various phenotypes and finally cell death. A snapshot of hyphae thus will show a mixture of normal and severely impaired hyphae and all stages in between (Fig. 5B and C). However, most of the phenotypic effects of the *katA* deletion are related to polar growth and the cytoskeleton: cell wall and septum formation, nuclear distribution, germ tube formation and branching. A third possibility is that KatA participates in the structure of the SPB, because of its proximity during interphase. As a result of its deletion there is a cytoskeletal disruption that affects polar growth and generates the described aberrant forms.

The protein sequence of KatA is only very weakly conserved in higher eukaryotes but the localization at kinetochores strengthens the idea that it is a homologue of CENP-H. It was proposed that CENP-E links spindle microtubules to kinetochores (Yao *et al*., 2000), but none of the interacting partners identified functions at the inner kinetochore plate. Assuming that KatA is a homologue of CENP-H, we identified KipA as an interacting partner. This suggests CENP-E as an interacting partner of CENP-H in higher eukaryotes. In agreement with this hypothesis is that depletion of CENP-H by RNAi reduced CENP-E binding to the kinetochore to 72% in human cells (Orthaus *et al*., 2006). Another connection between CENP-H and E is established through the protein Nuf2, a member of the tetrameric complex Ndc80, which can bind both CENP-H (Mikami *et al*., 2005) and CENP-E (Liu *et al*., 2007).

If KipA fulfils the same function in *A. nidulans* than CENP-E in vertebrates, it has to be considered, that the coiled-coil region of CENP-E is very long (230 nm) and could span the distance between the spindle microtubules and the kinetochore inner plate. The KipA coiled-coil domain is considerably shorter than the one of CENP-E and a function as centromere-kinetochore linker seems to be unlikely in fungi. However, the structure of the fungal kinetochore is clearly different from that of higher eukaryotes. All eight kinetochores form a single cluster and there are exclusive fungal complexes like the Dam–DASH ring, which bind KipA too (see below and Table 1). On the other hand, CENP-E acts as regulator of the checkpoint activity (Weaver *et al*., 2003). We do have further results that suggest such a function also in *A. nidulans*. We identified other kinetochore-associated proteins (Table 1), such as AN2768 and AN2054, in the yeast two-hybrid screening. The first one was SpcA a well-conserved fungal protein integrated in the DASH complex that forms a ring around the microtubule lattice at the kinetochore (Miranda *et al*., 2005). SpcA was located at the kinetochore during mitosis and the GFP–SpcA signal overlapped with that of mRFP1–KatA (Fig. 4B). The interaction between KipA and SpcA suggests that the Dam–DASH ring could be pulled along microtubules by the kinesin or that it participates as a tension sensor. The second one is very similar to mammalian haspin and less similar to yeast Alk1 and Alk2 (Nespoli *et al*., 2006). We named it AlkA and it localizes in the nucleus during mitosis (Fig. S2). Haspin is a kinase that phosphorylates the centromeric histone H3 and is required for normal mitosis (Dai *et al*., 2006). At the centromeric nucleosome the histone H3 is replaced by CENP-A, which is closely associated to the CENP-H complex (Okada *et al*., 2006). Again, we have another possible relationship between KipA and KatA indirectly through AlkA. Taking these data together, we propose that KipA is implicated in the control of the kinetochore-centromere attachment in fungi, like CENP-E in higher eukaryotes. In agreement with such a role for KipA is also the recent finding that CENP-H, as part of the CENP-A NAC/CAD complex, has been proposed to be a direct regulator of kinetochore-microtubule dynamics (Amaro *et al*., 2010).

In vertebrates, the kinesin CENP-E localized to the outer kinetochores and is essential for the establishment and correct functioning of the spindle checkpoint (Putkey *et al*., 2002). The spindle associated checkpoint arrests mitosis in metaphase until all kinetochores are correctly attached to microtubules. It was previously described in *A. nidulans* a hypersensitivity to microtubule destabilization of *sldA744* mutants (Efimov and Morris, 1998). *SldA* is the homologue of the budding yeast spindle assembly checkpoint gene *BUB1.* A *ΔkipA* mutant is also more sensitive to benomyl than wild-type and it was also suggested a redundant function of KipA and the mitotic kinesin KipB (Konzack *et al*., 2005). In the diploid strains, the number of haploidization sectors was only at low concentrations of benomyl slightly higher in the *ΔkipA/ΔkipA* mutant than in the wild-type (Fig. 7C). This indicates that the absence of KipA produces a slight increase in aneuploidy events, suggesting a small role in the kinetochore similar to CENP-E in vertebrates. Deletion of *kipA* in *A. nidulans* results in a curved-hyphal phenotype but the colony phenotype is not altered (Konzack *et al*., 2005 and Fig. 5A). It is surprising that altered polar growth has no effect on the colony size. However, *A. nidulans* strains with an inactive spindle assembly checkpoint display a faster mitosis than wild-type (De Souza *et al*., 2009). If KipA is necessary for this checkpoint activity, like CENP-E, the deletion of *kipA* should result in faster nuclear divisions and probably faster growth that could compensate the longer distance of a curved hypha.

Our investigation of the localization of AlpA at the mitotic spindle provides evidence for a new function of AlpA after metaphase. It was proposed that Alp14, the homologue of AlpA in *S. pombe*, localizes at the kinetochore in metaphase and is responsible for the activation of the checkpoint (Garcia *et al*., 2001). Our results suggest that in the moment the kinetochores divide and segregate to the poles, AlpA migrates to the kinetochores and moves polewards together with them (Fig. 3B, anaphase). AlpA is still observable at the kinetochore in telophase while KipA has disappeared completely from the spindle (Fig. S6). Recently, it was proposed that XMAP215, the *Xenopus* homologue, is a microtubule polymerase and promotes microtubule growth (Brouhard *et al*., 2008). This activity is reversible and XMAP215 can also accelerate microtubule depolymerization. In addition, it has been reported that Alp14/Dis1 and the microtubule-destabilizing kinesin Klp5/Klp6 play cooperative roles in *S. pombe* and the double knock-out is synthetically lethal (Garcia *et al*., 2002). We propose that the role of AlpA in mitosis is related to microtubule dynamics, promoting anaphase depolymerization of the spindle microtubules, and not to the checkpoint activity. On the contrary, it may be that the kinetochore components switch AlpA from a microtubule-stabilizing protein to a depolymerase at the end of metaphase.

In summary, KipA is a kinesin-7 motor protein with two faces: a previously reported role in polar growth and a new role during mitosis related to that of CENP-E.

Experimental procedures

Strains, plasmids and culture conditions

Supplemented minimal (MM) and complete media (CM) for *A. nidulans* were prepared as described, and standard strain construction procedures are described by Hill and Käfer (2001). A list of *A. nidulans* strains used in this study is given in Table 2. Standard laboratory *Escherichia coli* strains (XL-1 blue, Top 10 F′) were used. Plasmids are listed in Table 3.

Molecular techniques

Standard DNA transformation procedures were used for *A. nidulans* (Yelton *et al*., 1984), *E. coli* (Sambrook and Russel, 1999) and *S. cerevisiae*. For PCR experiments, standard protocols were applied using a Biometra Personal cycler (Biometra, Göttingen) for the reaction cycles. DNA sequencing was done commercially (eurofins-MWG-operon, Ebersberg, Germany). Genomic DNA was extracted from *A. nidulans* with the DNeasy Plant Mini Kit (Qiagen, Hilden, Germany). DNA analyses (Southern hybridizations) were performed as described by Sambrook and Russel (1999). Western blot was performed with the MiniProtean system (Bio-Rad) following the manufacturer instructions.

Deletion of katA

katA flanking regions were amplified by PCR using genomic DNA and the primers Kat1.2 (5′-AGGAATGTTTTCGA GGTTAGC-3′) and pyrG–KatA–LB (5′-gaagagcattgtttgaggc gAGAGCAAGGCCTCGTGGCAGG-3′) for the upstream region of *katA* and pyrG–KatA–RB (5′-atcagtgcctcctctcagac agTGCGGTACAGGGATATTTTGG-3′) and kat3 (5′-ACCGC CCAGATGGAGCTGGTC-3′) for the downstream. The *pyrG*-gene from plasmid pFNO3 (S. Osmani, Ohio, USA) was amplified by PCR and used as template together with katA-flanking regions for the fusion-PCR. The deletion cassette was amplified with the fusion-PCR method (Szewczyk *et al*., 2006) with the primers kat1.2 and kat3. The resulting PCR-product was transformed into the *pyrG89*-auxotrophic *A. nidulans* strain SO451 (kindly provided by S. Osmani, Ohio State University, USA) and the transformants were selected by the heterokaryon rescue method (Osmani *et al*., 2006a).

Transformants were screened by PCR for the homologous integration event. Single integration of the construct was confirmed by Southern blotting (Fig. S3). One *katA* deletion strain was selected from the transformants and named SSH29.

Tagging of proteins with GFP

For fluorescence microscopy a 0.3 kb fragment of the *katA* gene and the full length of *spcA*, respectively, were cloned into two versions of the pCMB17apx plasmid one with GFP as tag and *pyr4* as marker, and the other one with mRFP1 and *pyroA*. The resulting plasmids are listed in Table 1. The primer set used for *katA* was AN2886-AscI (5′-GGCGCGCCTATGACA

Table 2. *A. nidulans* strains used in this study.

Strain	Genotype	Source
TN02A3	*pyrG89; argB2, ΔnkuA::argB; pyroA4*	Nayak *et al.* (2006)
RMS011	*pabaA1, yA2; ΔargB::trpCΔB; trpC801, veA1*	Stringer *et al.* (1991)
SJW02	*wA3; pyroA4; alcA(p)::GFP::tubA; ΔargB::trpCΔB*	J. Warmbold, Marburg, Germany
SSK44	*pabaA1; wA3; ΔargB::trpCΔB; ΔkipA::pyr4; veA1* (Δ*kipA*)	Konzack *et al.* (2005)
SSK92	*wA3; pyroA4; alcA(p)::GFP::kipA*	Konzack *et al.* (2005)
SSK28	*pabaA1; wA3*; Δ*kipB::argB; pyroA4*, Δ*kipA::pyr4*	Konzack *et al.* (2005)
SCE05	*ΔargB::trpCΔB; pyroA4; alcA(p)::GFP::alpA*	Enke *et al.* (2007)
SDV83	*pabaA1, yA2, pyrG89; ΔalpA::pyr4*	Enke *et al.* (2007)
SNZ59	TN02A3 transformed with pNZ-SI38 [*apsB(p)::GFP::apsB*]	N. Zekert. Karlsruhe, Germany
SO451	*pyrG89; wA3; argB2; pyroA4; ΔnkuA::argB; sE15, nirA14, chaA1, fwA1*	Nayak *et al.* (2006)
CDS394	*wA3; argB2; pyroA4; Nup49::GFP::pyrG*	Osmani *et al.* (2006b)
SSH03	TN02A3 transformed with pSH17 (GFP-AlkA) *pyroA4*	This study
SSH04	TN02A3 transformed with pSH18 (GFP–KatA) *pyroA4*	This study
SSH08	TN02A3 transformed with pNT (YFP^N–KatA) and pNT36 (YFP^C–KipA) *pyroA4*	This study
SSH11	SSK44 *(ΔkipA*) crossed to SSH04 (GFP–KatA) *wA3*	This study
SSH15	TN02A3 transformed with pSH32 (mRFP1-AlkA) *pyrG89*	This study
SSH16	TN02A3 transformed with pSH33 (mRF1P–KatA) *pyrG89*	This study
SSH17	SJW02 (GFP–TubA) crossed to SSH15 (mRFP1-AlkA)	This study
SSH18	SJW02 (GFP–TubA) crossed to SSH16 (mRFP1–KatA)	This study
SSH20	SCE05 (GFP–AlpA) crossed to SSH16 (mRFP1–KatA)	This study
SSH24	SNZ59 (GFP–ApsB) crossed to SSH16 (mRFP1–KatA)	This study
SSH25	SSK92 (GFP–KipA) crossed to SSH16 (mRFP1–KatA)	This study
SSH26	CDS394 (GFP–Nup49) crossed to SSH16 (mRFP1–KatA)	This study
SSH27	SSK92 (GFP–KipA) crossed to RMS011; *wA3, yA2, ΔargB::trpC ΔB*	This study
SSH29	SO451 transformed with the *katA* deletions cassette. *wA3; pyrG89; argB2; pyroA4, ΔnkuA::argB; sE15; ΔkatA::pyrG*	This study
SSH31	SSH27 (GFP–KipA) crossed to SSH29 (ΔkatA)	This study
SSH32	SJW02 (GFP–TubA) transformed with pSH34 (mRFP1–KipA) *wA3, ΔargB::trpCΔB; trpC801*	This study
SSH33	SSH32 (GFP–TubA) crossed to SSH29 (ΔkatA) *wA3*	This study
SSH34	TN02A3 transformed with pSH21 (GFP-Spc34); *argB2, ΔnkuA::argB; pyroA4; alcA(p)::GFP::spcA*	This study
SSH38	SSH16 (mRFP1–KatA) crossed to SSH34 (GFP-spc34)	This study
SSH46	TN02A3 transformed with pSH42 (3xHA–KatA) *argB2, ΔnkuA::argB; pyrG89; alcA(p)::3xHA::katA*	This study
SSH47	SSH27 (GFP–KipA) crossed to SSH46 (HA–KatA); *yA2*	This study
SSH48	Diploid strain *katA/katA* of cross between SO451 x RMS011	This study
SSH49	Diploid strain *katA/ΔkatA* of cross between SSH29 x RMS011	This study
SSH50	SSK44 crossed to RMS011, *yA2, ΔkipA, ΔargB::trpCΔB, trpC801*	This study
SSH51	SSH58 crossed to RMS011; *yA2; ΔkipA, pyroA4*	This study
SSH52	TN02A3 transformed with katA-GFP cassette; *katA(p)::katA::GFP; argB2, ΔnkuA::argB; pyroA4*	This study
SSH58	SSK44 *(ΔkipA*) crossed to GR5; *wA3, ΔkipA, pyroA4*	This study
SSH59	*kipA/kipA* diploid strain from cross of GR5 to RMS011	This study
SSH60	*ΔkipA/ΔkipA* diploid strain from cross of SSH51 to SSK44	This study
SSH61	*Δ kipA/kipA* diploid strain from cross of SSK44 to RMS011	This study

All strains harbour in addition the *veA1* mutation. In strains used for crosses only the relevant mutation are listed.

TCTTCCAAAGGGCG) and AN2886-PacI (5′-TTAATTAATAA TGAGCACGGTGCTGACCG). The restiction sites *Asc*I and *Pac*I are underlined. For *spcA* the primer set was AN2768-Asc (5′-ATACCAAAAGGCGCGCCGATGTCGTTGCTAGAAAGC CAC) and Spc34-rev-pac2 (5′-TTAATTAATCACGAAAGG CCGCCCAAATC). All of these plasmids were transformed into the uracil-auxotrophic TN02A3 (Δ*nkuA*). The integration events were confirmed by PCR and Southern blotting (results not shown).

Yeast two-hybrid analysis

The yeast two-hybrid analysis was performed using the Matchmaker Library Construction & Screening system (BD Clontech). For bait generation, a *kipA* cDNA fragment corresponding to the C-terminal half of KipA (505-889 amino acids) with primers KipA-F(NcoI) (5′-CCATGGATTCGCTGGTC AGTATTCTTTG) and KipA_SR (5′-GCGCGTCGACTCATG CACTTGGACGACTG-3′) was amplified and cloned in the pGBKT7 vector, which contains the GAL4 DNA-BD and the *TRP1* marker (BD Clontech). cDNA from *Aspergillus* strain SRF200 were amplified and cloned in the pGADT7-Rec vector, under the manufacturer instructions, which contains the GAL4 DNA-AD and the *LEU2* marker (BD Clontech). pGBK7-associated plasmids were transformed in yeast AH109 (mating type *MAT*a) and pGADT7-associated plasmids were transformed in yeast Y187 (mating type *MAT*α). The system utilizes two reporter genes (*HIS3* and *LacZ*) under the

Table 3. Plasmids used in this study.

Plasmids	Construction	Source
pCR2.1-TOPO	Cloning vector	Invitrogen (NV Leek, The Netherlands)
pCMB17apx	*alcA(p)::GFP*, for N-terminal fusion of GFP to proteins of interest; contains *N. crassa pyr4*	V. Efimov (Piscataway, USA)
pGBKT7	Yeast Two-Hybrid bait vector, Gal4-BD	Clontech
pGADT7	Yeast Two-Hybrid prey vector, Gal4-AD	Clontech
pDV7	GFP replaced N-terminal half of YFP in pCMB17apx	Takeshita *et al.* (2008)
pDV8	GFP replaced C-terminal half of YFP in pCMB17apx	Takeshita *et al.* (2008)
pCE05	*alpA* in pMT-mRFP1	Enke *et al.* (2007)
pSH09	1.1 kb *kipA* C-terminal fragment in pGBKT7	This study
pSH17	0.7 kb *alkA* fragment in pGBKT7apx	This study
pSH18	0.3 kb *katA* fragment in pCMB17apx	This study
pSH21	*spcA* (full length) in pCMB17apx	This study
pSH25	*kipA* deletion KW2 in pSH09	This study
pSH26	*kipA* deletion KW3 in pSH09	This study
pSH27	*kipA* deletion KW4 in pSH09	This study
pSH28	*kipA* fragment from pSH34 in pDV7	This study
pSH29	*katA* fragment from pSH18 in pDV8	This study
pSH32	0.7 kb *alkA* fragment in pCMB17apx, with mRFP1 instead of GFP and *pyroA* instead of *pyr4*	This study
pSH33	0.3 kb *katA* fragment in pCMB17apx, with mRFP1 instead of GFP and *pyroA* instead of *pyr4*	This study
pSH34	1.0 kb 5′-fragment of *kipA* in pCMB17 apx with mRFP1 instead of GFP and *pyroA* instead of *pyr4*	This study
pSH42	0.3 kb 5′-fragment of *katA* in pCMB17 apx with 3xHA instead of GFP and *pyroA* instead of *pyr4*	This study

control of the GAL4-responsive UAS. β-Galactosidase activity was analysed by colony-lift filter assay using X-gal (X-nitrophenyl β-D-galactopyranoside (Karl Roth) as substrate.

For the truncated versions of KipA used in the yeast two-hybrid assay, primers with phosphorylated 5′-ends were used to amplify the entire bait vector except the deleted region. The primers used for the KW2 mutant were KW2F (P-5′-GATGGAAAGGCGAGTGCTCAA) and KW1R (P-5′-AAGCTCTTTCTCGGCCTGCGC; for the KW3 were KW3F (P-5′-AACCAATCGTTACCAAAAGAG) and KW2R (P-5′-GTGGAATTCTTGGCTATGGAC); and for the KW4 were KW4F (P-5′-TAAGTCGACCTGCAGCGGCCG) and KW3R (P-5′-GGAGCGAAGAGCTGTCAGCAT).

Light/fluorescence microscopy

For live-cell imaging of germlings and young hyphae, cells were grown on coverslips in 0.4 ml MM + 2% glycerol (induction of the *alcA* promoter), MM + 2% glucose (repression of the *alcA* promoter). Cells were incubated at room temperature for 1–2 days. For pictures of young hyphae of each gene deletion strain, the spores were inoculated on microscope slides coated with MM + 2% glucose + 0.8% agarose and grown at 30°C for 1 day. Images were captured at room temperature using an Axiophot microscope (Zeiss, Jena, Germany). Images were collected and analysed with the AxioVision system (Zeiss).

Acknowledgements

We kindly thank Aysha and Stephen Osmani (Ohio State University, USA) and their colleagues for their help with the heterokaryon rescue technique and the generous gift of various plasmids and strains. This work was supported by the special program ‘Lebensmittel und Gesundheit’ from the Baden-Württemberg Stiftung. N.T. was a fellow of the Humboldt Society.

References

Amaro, A.C., Samora, C.P., Holtackers, R., Wang, E., Kingston, I.J., Alonso, M., *et al.* (2010) Molecular control of kinetochore-microtubule dynamics and chromosome oscillations. *Nat Cell Biol* **12:** 319–329.

Bieling, P., Laan, L., Schek, H., Munteanu, E.L., Sandblad, L., Dogterom, M., *et al.* (2007) Reconstitution of a microtubule plue-end tracking system *in vitro*. *Nature* **450:** 1100–1105.

Brouhard, G.J., Stear, J.H., Noetzel, T.L., Al-Bassam, J., Kinoshita, K., Harrison, S.C., *et al.* (2008) XMAP215 is a processive microtubule polymerase. *Cell* **132:** 79–88.

Brown, K.D., Coulson, R.M., Yen, T.J., and Cleveland, D.W. (1994) Cyclin-like accumulation and loss of the putative kinetochore motor CENP-E. *Dev Cell* **3:** 351–365.

Browning, H., Hayles, J., Mata, J., Aveline, L., Nurse, P., and McIntosh, J.R. (2000) Tea2p is a kinesin-like protein required to generate polarized growth in fission yeast. *J Cell Biol* **151:** 15–27.

Browning, H., Hackney, D.D., and Nurse, P. (2003) Targeted movement of cell end factors in fission yeast. *Nat Cell Biol* **5:** 812–818.

Busch, K.E., Hayles, J., Nurse, P., and Brunner, D. (2004) Tea2p kinesin is involved in spatial microtubule organization by transporting tip1p on microtubules. *Dev Cell* **16:** 831–843.

Carvalho, P., Gupta, M.L.J., Hoyt, M.A., and Pellman, D. (2004) Cell cycle control of kinesin-mediated transport of Bik1 (CLIP-170) regulates microtubule stability and dynein activation. *Dev Cell* **6:** 815–829.

Chan, G.K., Schaar, B.T., and Yen, T.J. (1998) Characterization of the kinetochore binding domain of CENP-E reveals interactions with the kinetochore proteins CENP-F and hBUBR1. *J Cell Biol* **143:** 49–63.

Dai, J., Sullivan, B.A., and Higgins, J.M.G. (2006) Regulation of mitotic chromosome cohesion by haspin and aurora B. *Dev Cell* **11:** 741–750.

De Souza, C.P., Hashmi, S.B., Nayak, T., Oakley, B., and Osmani, S.A. (2009) Mlp1 Acts as a Mitotic Scaffold to Spatially Regulate Spindle Assembly Checkpoint Proteins in *Aspergillus nidulans*. *Mol Biol Cell* **20:** 2146–2159.

Efimov, V.P., and Morris, N.R. (1998) A screen for dynein synthetic lethals in *Aspergillus nidulans* identifies spindle assembly checkpoint genes and other genes involved in mitosis. *Genetics* **149:** 101–116.

Enke, C., Zekert, N., Veith, D., Schaaf, C., Konzack, S., and Fischer, R. (2007) *Aspergillus nidulans* Dis1/XMAP215 protein AlpA localizes to spindle pole bodies and microtubule plus ends and contributes to growth directionality. *Eukaryot Cell* **6:** 555–562.

Fischer, R., Zekert, N., and Takeshita, N. (2008) Polarized growth in fungi – interplay between the cytosekelton, positional markers and membrane domains. *Mol Microbiol* **68:** 813–826.

Fukagawa, T., Mikami, Y., Nishihashi, A., Regnier, V., Haraguchi, T., Hiraoka, Y., *et al*. (2001) CENP-H, a constitutive centromere component, is required for centromere targeting of CENP-C in vertebrate cells. *EMBO J* **20:** 4603–4617.

Garcia, M.A., Vardy, L., Koonrugsa, N., and Toda, T. (2001) Fission yeast ch-TOG/XMAP215 hnomologue Alp14 connects mitotic spindles with the kinetochore and is a component of the Mad2-dependent spindle checkpoint. *EMBO J* **20:** 3389–3401.

Garcia, M.A., Koonrugsa, N., and Toda, T. (2002) Spindle–kinetochore attachment requires the combined action of Kin I-like Klp5/6 and Alp14/Dis1-MAPs in fission yeast. *EMBO J* **21:** 6015–5024.

Higashitsuji, Y., Herrero, S., Takeshita, N., and Fischer, R. (2009) The cell end marker protein TeaC is involved in both growth directionality and septation in *Aspergillus nidulans*. *Eukaryot Cell* **8:** 957–967.

Hill, T.W., and Käfer, E. (2001) Improved protocols for *Aspergillus* minimal medium: trace element and minimal medium salt stock solutions. *Fungal Genet Newsl* **48:** 20–21.

Kim, Y., Heuser, J.E., Waterman, C.M., and Cleveland, D.W. (2008) CENP-E combines a slow, processive motor and a flexible coiled coil to produce an essential motile kinetochore tether. *J Cell Biol* **181:** 411–419.

Konzack, S., Rischitor, P., Enke, C., and Fischer, R. (2005) The role of the kinesin motor KipA in microtubule organization and polarized growth of *Aspergillus nidulans*. *Mol Biol Cell* **16:** 497–506.

Liu, D., Zhang, N., Du, J., Cai, X., Zhu, M., Jin, C., *et al*. (2006) Interaction of Skp1 with CENP-E at the midbody is essential for cytokinesis. *Biochem Biophys Res Commun* **345:** 394–402.

Liu, D., Ding, X., Du, J., Cai, X., Huang, J., Ward, T., *et al*. (2007) Human NUF2 interacts with centromere-associated protein E and is essential for stable spindle microtubule-kinetochore attachment. *J Biol Chem* **282:** 21415–21424.

Liu, H.L., Souza, C.P.D., Osmani, A.H., and Osmani, S.A. (2009) The three fungal transmembrane nuclear pore complex proteins of *Aspergillus nidulans* are dispensable in the presence of an intact An-Nup84-120 complex. *Mol Biol Cell* **20:** 616–630.

Liu, X., McLeod, I., Anderson, S., Yates, J.R., and He, X. (2005) Molecular analysis of kinetochore architecture in fission yeast. *EMBO J* **24:** 2919–2930.

Meraldi, P., McAinsh, A.D., Rheinbay, E., and Sorger, P.K. (2006) Phylogenetic and structural analysis of centromeric DNA and kinetochore proteins. *Genome Biol* **7:** R23.

Mikami, Y., Hori, T., Kimura, H., and Fukagawa, T. (2005) The functional region of CENP-H interacts with the Nuf2 complex that localizes to centromere during mitosis. *Mol Biol Cell* **25:** 1958–1970.

Miranda, J.J., Wulf, P.D., Sorger, P.K., and Harrison, S.C. (2005) The yeast DASH complex forms closed rings on microtubules. *Nat Struct Mol Biol* **12:** 138–143.

Nayak, T., Szewczyk, E., Oakley, C.E., Osmani, A., Ukil, L., Murray, S.L., *et al*. (2006) A versatile and efficient gene targeting system for *Aspergillus nidulans*. *Genetics* **172:** 1557–1566.

Nespoli, A., Vercillo, R., Nola, L., Diani, L., Giannattasio, M., Plevanti, P., and Muzi-Falconi, M. (2006) Alk1 and Alk2 are two novel cell cycle-regulated haspin-like proteins in the budding yeast. *Cell Cycle* **5:** 1464–1471.

Okada, M., Cheeseman, I.M., Hori, T., Okawa, K., McLeod, I.X., Yates, J.R., *et al*. (2006) The CENP-H-I complex is required for the efficient incorporation of newly sythesized CENP-A into centromeres. *Nat Cell Biol* **8:** 446–457.

Orthaus, S., Ohndorf, S., and Diekmann, S. (2006) RNAi knockdown of human kinetochore protein CENP-H. *Biochem Biophys Res Commun* **348:** 36–46.

Osmani, A., Oakley, B.R., and Osmani, S.A. (2006a) Identification and analysis of essential Aspergillus nidulans genes using the heterokaryon rescue technique. *Nat Protoc* **1:** 2517–2526.

Osmani, A.H., Davies, J., Liu, H.L., Nile, A., and Osmani, S.A. (2006b) Systematic deletion and mitotic localization of the nuclear pore complex proteins of *Aspergillus nidulans*. *Mol Biol Cell* **17:** 4946–4961.

Pidoux, A.L., Richardson, W., and Allshire, R.C. (2003) Sim4: a novel fission yeast kinetochore protein required for centromeric silencing and chromosome segregation. *J Cell Biol* **161:** 295–307.

Przewloka, M.R., and Glover, D.M. (2009) The kinetochore and the centromere: a working long distance relationship. *Annu Rev Genet* **43:** 439–465.

Putkey, F.R., Cramer, T., Morphew, M.K., Silk, A.D., Johnson, R.S., McIntosh, J.R., and Cleveland, D.W. (2002) Unstable kinetochore-microtubule capture and chromosomal instability following deletion of CENP-E. *Dev Cell* **3:** 351–365.

Rischitor, P., Konzack, S., and Fischer, R. (2004) The Kip3-like kinesin KipB moves along microtubules and determines spindle position during synchronized mitoses in *Aspergillus nidulans* hyphae. *Eukaryot Cell* **3:** 632–645.

Sambrook, J., and Russel, D.W. (1999) *Molecular Cloning: A Laboratory Manual*. Cold Spring Harbor, NY: Cold Spring Harbor Laboratory Press.

Sanchez-Perez, I., Renwick, S.J., Crawley, K., Karig, I.,

Buck, V., Meadows, J.C., *et al*. (2005) The DASH complex and Klp5/Klp6 kinesin coordinate bipolar chromosome attachment in fission yeast. *EMBO J* **24:** 2931–2943.
Schliwa, M., and Woehlke, G. (2003) Molecular motors. *Nature* **422:** 759–765.
Sharpless, K.E., and Harris, S.D. (2002) Functional characterization and localization of the *Aspergillus nidulans* formin SEPA. *Mol Biol Cell* **13:** 469–479.
Snaith, H.A., and Sawin, K.E. (2003) Fission yeast mod5p regulates polarized growth through anchoring of tea1p at cell tips. *Nature* **423:** 647–651.
Snaith, H.A., Samejima, I., and Sawin, K.E. (2005) Multistep and multimode cortical anchoring of tea1p at cell tips in fission yeast. *EMBO J* **24:** 3690–3699.
Stringer, M.A., Dean, R.A., Sewall, T.C., and Timberlake, W.E. (1991) *Rodletless*, a new *Aspergillus* developmental mutant induced by directed gene inactivation. *Genes Dev* **5:** 1161–1171.
Szewczyk, E., Nayak, T., Oakley, C.E., Edgerton, H., Xiong, Y., Taheri-Talesh, N., *et al*. (2006) Fusion PCR and gene targeting in *Aspergillus nidulans*. *Nat Protoc* **1:** 3111–3120.
Takeshita, N., Higashitsuji, Y., Konzack, S., and Fischer, R. (2008) Apical sterol-rich membranes are essential for localizing cell end markers that determine growth directionality in the filamentous fungus *Aspergillus nidulans*. *Mol Biol Cell* **19:** 339–351.
Veith, D., Scherr, N., Efimov, V.P., and Fischer, R. (2005) Role of the spindle-pole body protein ApsB and the cortex protein ApsA in microtubule organization and nuclear migration in *Aspergillus nidulans*. *J Cell Sci* **118:** 3705–3716.
Wang, H.W., Ramey, V.H., Westermann, S., Leschziner, A.E., Welburn, J.P.I., Nakajima, Y., *et al*. (2007) Architecture of the Dam1 kinetochore ring complex and implications of microtubule-driven assembly and force-coupling mechanisms. *Nat Struct Mol Biol* **14:** 721–726.
Weaver, B.A.A., Bonday, Z.Q., Putkey, F.R., Kops, G.J.P.L., Silk, A.D., and Cleveland, D.W. (2003) Centromere-associated protein-E is essential for the mammalian mitotic checkpoint to prevent aneuploidy due to single chromosome loss. *J Cell Biol* **162:** 551–563.
Wickstead, B., and Gull, K. (2006) A 'Holistic' kinesin phylogeny reveals new kinesin families and predicts protein functions. *Mol Biol Cell* **17:** 1734–1743.
Wu, X., Xiang, X., and Hammer, J.A. III (2006) Motor proteins at the microtubule plus-end. *Trends Cell Biol* **16:** 135–143.
Yang, L., Ukil, L., Osmani, A., Nahm, F., Davies, J., Souza, C.P.C.D., *et al*. (2004) Rapid production of gene replacement constructs and generation of a green fluorescent protein-tagged centromeric marker in *Aspergillus nidulans*. *Eukaryot Cell* **3:** 1359–1362.
Yao, X., Anderson, K.L., and Cleveland, D.W. (1997) The microtubule-dependent motor centromere-associated protein E (CENP-E) is an integral component of kinetochore corona fibers that link centromeres to spindle microtubules. *J Cell Biol* **139:** 435–447.
Yao, X., Abrieu, A., Zheng, Y., Sullivan, K.F., and Cleveland, D.W. (2000) CENP-E forms a link between attachment of spindle microtubules to kinetochores and the mitotic checkpoint. *Nat Cell Biol* **2:** 484–491.
Yelton, M.M., Hamer, J.E., and Timberlake, W.E. (1984) Transformation of *Aspergillus nidulans* by using a *trpC* plasmid. *Proc Natl Acad Sci USA* **81:** 1470–1474.
Zhu, M., Wang, F., Yan, F., Yao, P.Y., Du, J., Gao, X., *et al*. (2008) Septin 7 interacts with the centromere-associated protein E and is required for its kinetochore localization. *J Biol Chem* **283:** 18916–18925.

Supporting information

Additional supporting information may be found in the online version of this article.

Please note: Wiley-Blackwell are not responsible for the content or functionality of any supporting materials supplied by the authors. Any queries (other than missing material) should be directed to the corresponding author for the article.